J Biol Phys (2006) 32:465–472
DOI 10.1007/s10867-006-9029-5

RESEARCH PAPER

Managing Free-energy Barriers in Nuclear Pore Transport

Brian Nielsen · Claus Jeppesen · John H. Ipsen

Received: 7 April 2006 / Accepted: 12 November 2006 /
Published online: 19 December 2006
© Springer Science + Business Media B.V. 2006

Abstract The Nuclear Pore Complexes (NPC) facilitate highly selective gateways for transport of macromolecules across the Nuclear Envelope (NE). Based on the current accumulated knowledge of the architecture of NPC we have established a minimal physical model of the pore and the transport mechanism. The barrier properties of the NPC model are analyzed by the recently established Wang–Landau Monte Carlo computer simulation technique and the transport properties are extracted by employing Kramers' theory of reaction rates. We show that our physical model can account for a range of characteristics observed for nuclear pore transport.

Key words nuclear pore · cellular transport · random walk · entropic sampling

1 Introduction

The mechanism for active transport of macromolecules through NPC remains poorly understood, despite the rapid advances in our knowledge of the architecture and molecular components of NPC. It has been known for some time that macromolecules (cargo) require the presence of a short peptide sequence, The Nuclear Localization Sequence (NLS), for transport through NPC into the nucleus. Further, the presence of transport proteins importin α and β which associate with the NLS-bearing macromolecule by RanGDP in cytoplasm, while RanGTP dissociates the complex in nucleoplasm. Similarly, macromolecules with a Nuclear Export Sequence (NES) and proteins exportin α and β are required for active transport of macromolecules out of the nucleus. A range of other carrier proteins has been found, but to keep the discussion simple we will only refer to transport from cytoplasm to nucleoplasm

B. Nielsen · C. Jeppesen · J. H. Ipsen (✉)
Department of Physics, MEMPHYS—Centre for Biomembrane Physics, Syddansk Universitet, Campusvej 55, DK-5230 Odense, Denmark
e-mail: ipsen@memphys.sdu.dk

and nominate the transport protein as the carrier, which, together with RanGDP and cargo, form a cargo-carrier complex [1]. NPC is embedded in NE, a continuous elastic composite shell structure consisting of two lipid membranes and lamin protein meshwork surrounding the nucleus [2]. The structure of the NPC is particularly well documented for nuclei of yeast (*Saccharomyces cerevisia*) where all the nucleoporins (Nups) involved have been mapped out [3]. It is comprised of only 30 Nups localized in NPC with large molecular weight ($\sim$ 60 MDa), and has an inner diameter of $\sim$ 45 nm, while the length of the pore stretches about 90 nm. NPC has an eightfold rotation symmetry around an axis normal to NE and an approximate symmetry with respect to the mid-plane of NE. It is striking that a third of the NPC mass is constituted by multiple copies of 13 different Nups, which are rich in phenylaline and glycine. These FG-Nups lack secondary structure [4], with Stokes' radii in solution up to 10 nm [5] and act as binding sites for the cargo-carrier complex, reviewed in [6]. Also, it is noteworthy that no molecular motors or other enzymes associated with transport are located in NPC. Rather, single-molecule detection of actively transported gold particles appears to conduct completely random motion in the pore [7]. This structure is an effective barrier for large particles, 25 nm in diameter for gold particles, while particles smaller than 9 nm pass freely [8, 9].

2 Model

The experimental findings suggest that the FG-Nups play a pivotal role in active nuclear pore transport. In our model description the FG-Nups are represented as flexible polymers grafted to a hole in an impenetrable wall, modeling the nuclear pore in NE. The absence of motor proteins and random motion of particles in NPC suggest a model based on simple diffusive transport over the barrier set by the FG-Nups. In this respect our physical model has similarities with the biological "Brownian gating model" [3] and aspects of other biological and physical models for nuclear pore transport [6, 10–13]. The description of the transport of the cargo-carrier complex through NPC therefore takes its beginning in Kramers' "reaction rate" theory [14] which deals with transport of Brownian particles over a barrier. In the overdamped system this is described by Smolouchovsky's equation

$$\frac{\partial P(l,t)}{\partial t} = D\frac{\partial}{\partial l}\left(\frac{1}{k_B T}\frac{\partial F(l)}{\partial l} + \frac{\partial}{\partial l}\right)P(l,t). \tag{1}$$

l is here the "reaction coordinate" representing the position of the cargo-carrier complex through the NPC, and $P(l,t)$ is the associated time-dependent probability distribution. Equation (1) can be evaluated from first principles assuming that the dynamics of l is slow compared to the characteristic time scales of the solvent molecules and the components, which constitute the barrier [15]. This condition is fulfilled since the radial relaxation time for random coiled polypeptides is in the μsec range [16] while the passive diffusion of macromolecules over length scales of the NPC is a msec phenomenon. Such an approach shows that $F(l)$ is the free energy of the total system constrained to a particular value of l. D is the diffusion constant of the cargo-carrier complex. The rate of transport from cytoplasm to nucleoplasm $k_{C\to N}$ is then the inverse of the mean exit time [17] from the pore at steady state obtained from (1) for absorbing boundary conditions at l_N on the nucleoplasmic side,

representing the rapid disassembly of the cargo-complex catalyzed by RanGTP and nuclear porins associated with the nuclear basket [18, 19]. It can be derived from Eq. (1) as

$$k_{C\to N} = \frac{D}{\int_{l_C}^{l_N} dl \exp\left(-\frac{F(l)}{k_B T}\right) \int_{l_C}^{l} dl' \exp\left(\frac{F(l')}{k_B T}\right)}, \tag{2}$$

where l_C is some position close to the pore at the cytoplasmic side. The form of $F(l)$ is evaluated from a minimal model of NPC where NE is described as an impenetrable wall perforated by a hole. We have implemented two versions of the model. In the first (Figure 1a), the pore is half-torus shaped and decorated with flexible string and bead polymers grafted in the center of the pore, representing the FG-Nups, while in the second (Figure 1b), the pore is cylinder-shaped with the flexible polymers end-grafted at the two ends of the cylinder. The model b) is closer to the actual architecture of the NPC, while the former is included to demonstrate the generality of the principle. The cargo-carrier complexes are represented by small polymers of varying size, where one monomer has some affinity $\epsilon \sim -k_B T$ to the monomers of the FG-Nups when they are within some small cut-off distance. The barrier is dividing a box, which defines the total system. The form of $F(l)$ is obtained via entropic sampling [20] by Wang–Landau Monte Carlo computer simulation techniques [21] which enable a numerical determination of the density of states $\rho(l, E)$:

$$F(l) = -k_B T \ln\left(\sum_E \rho(l, E) \exp\left(-\frac{E}{k_B T}\right)\right), \tag{3}$$

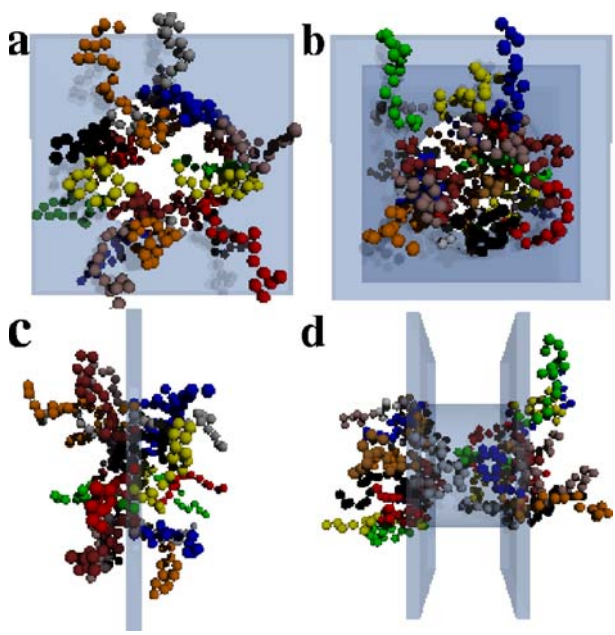

Figure 1 The model of NPC in NE is represented as a pore through an impenetrable wall (*blue*) and the FG-Nups are described as flexible polymers end-grafted in the pore, which is here shown in *front and side views*. **(a)** and **(c)**: String and bead polymers, representing FG-Nups, are evenly distributed in the *center of a half-torus shaped pore*. The dimensions of the pore used in the calculations are wall thickness 2.5, and inner diameter 27.5, in units of bead extent. **(b)** and **(d)**: FG-Nups are located evenly at the end of a *cylinder-shaped pore* through NE. The diameter is 27.5 and the total length is 22.5 in units of bead extent.

where E is the total interaction energy. This novel numerical technique thus allows for an accurate determination of the shape of $F(l)$, which is not accessible by traditional importance sampling Monte Carlo simulation techniques or molecular dynamics. In the present simulations, $\rho(l, E)$ is characterized by a 8–10·10^3-fold binning of l along the full length of the simulation box and E is a multiple of ϵ. The relative error in the determination of this discretized density of states is less than 0.1% within each bin [21].

3 Results and Discussion

The model can account for a range of observed characteristics of nuclear pore transport. The basic mechanism is illustrated in Figure 2, where it is shown that the presence of flexible FG-Nups gives rise to a large barrier for transport of large non-NLS-carrying ($\epsilon = 0$) objects. In general the barrier must be large enough to hinder the passive transport through NPC facilitated by the concentration gradient across NE. The barrier is steric-entropic, a well-known mechanism of repulsion between flexible polymers and lipid membranes where conformational entropy dominates the free energy. Since the barrier height is growing with the temperature due to its entropic origin, a standard experimental Arrhenius analysis of such a system will not provide information about the actual barrier height. The strong size-dependence of passive transport observed in experiments is accounted for in this model, since D is decreasing with the size of the macromolecule in solution according to the Stokes–Einstein relation and the barrier height is increasing with size as shown in Figure 3. This aspect of Nuclear Pore Transport was also captured in theoretical descriptions of the inner NPC as a reversible polymer gel [12, 13]. The presence of FG-Nups with some affinity to the cargo-carrier complex ($\epsilon < 0$) can reduce this barrier significantly (Figure 2) and thus allow for passage through the pore, and even lead to an attractive well at high interaction strengths. Within the framework of this

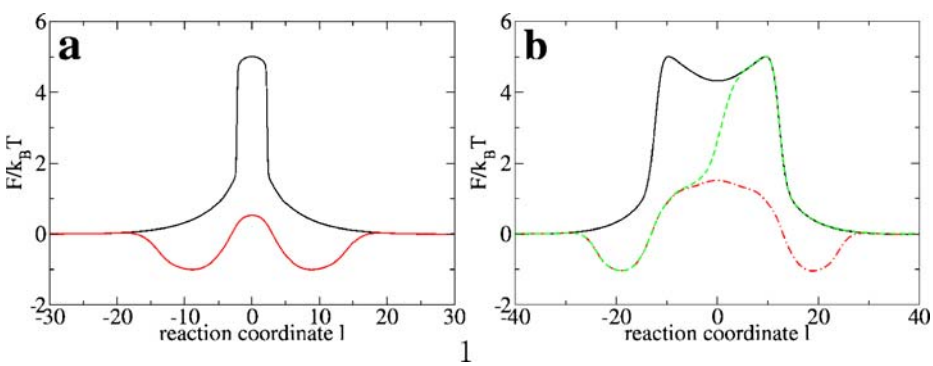

Figure 2 Barrier properties of two arrangements of FG-Nups in model NPC. **(a)** The FG-Nups, 24 polymers each with 16 monomers, are evenly distributed in the *center of the pore* with FG-Nups with $\epsilon = 0$ (*black line*) and FG-Nups with $\frac{\epsilon}{k_B T} = -4.0$ (*red line*). **(b)** FG-Nups, 16 polymers each with 16 monomers, are placed at each of the outer rims of the pore with symmetric distribution of FG-Nups with $\epsilon = 0$ (*black line*), symmetric distribution with $\frac{\epsilon}{k_B T} = -4.0$ (*red dashed-dotted line*), asymmetric distribution of FG-Nups, *left side* $\frac{\epsilon}{k_B T} = -4.0$, *right side* $\epsilon = 0$ (*dashed green*).

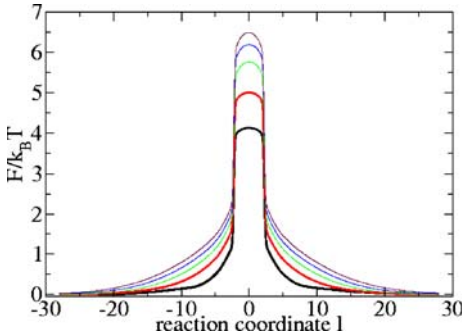

Figure 3 Barrier dependence on size of cargo-carrier complex. The simple pore (see Figure 1a,c) is equipped with 24 polymers, each with 16 mononers, representing the FG-Nups. The cargo-carrier size varies from 5 (*black curve*), 10 (*red*), 15 (*green*), 20 (*blue*) and 25 (*maroon*) monomers and $\epsilon = 0$. The barrier height is strongly increasing with the size of the cargo-carrier complex.

model, the observed multiple binding sites and fast binding events [1, 7, 22] help to provide a local polymeric solvent for cargo-carrier complexes in NPC. The barrier property of NPC is thus determined by an intricate interplay between polymer conformational entropy, steric factors, binding enthalpy and binding entropy.

The pore thus only allows for transport of macromolecules with affinity for the FG-Nups. However, the transport is most effective in a narrow range of interaction strength ϵ (Figure 4) making the transport highly selective. Figure 4a shows that the presence of non-binding FG-Nups among binding FG-Nups in NPC does not hinder the active transport of cargo-carrier complexes as long as the binding FG-Nups are distributed throughout the pore. The model thus allows for multiple independent transport pathways [1, 23], where a particular class of cargo-carrier complexes can

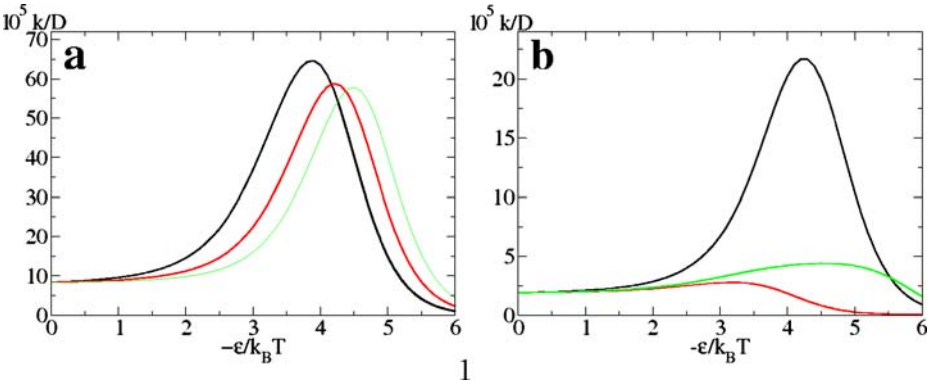

Figure 4 Reaction rates versus affinity ϵ for **(a)** centrally placed FG-Nups, represented by 24 polymers each with 16 monomers, where all FG-Nups have affinity for the cargo-carrier complex (*black curve*), or only 12 FG-Nups (*red*) or 6 FG-Nups (*green*) of the total 24 FG-Nups have affinity ($\epsilon < 0$) for the cargo-carrier complex. **(b)** For symmetrically distributed FG-Nups, modeled by 16 polymers per rim each with 16 monomers, (*black curve*), asymmetrically distributed FG-Nups with no affinity ($\epsilon = 0$) on the *left side* (*red*) and no affinity ($\epsilon = 0$) on the *right side* (*green*).

bind to some FG-Nups or regions of FG-Nups while other FG-Nups are non-binding [1]. Figure 4a also shows that for more binding sites for a cargo-carrier complex in NPC, the active transport gets more active and lower binding affinities are required. Experiments have shown that NPC devoid of FG-Nups symmetrically distributed between the cytoplasmic and nucleoplasmic side of NPC does not allow for active nuclear pore transport, while the asymmetrically distributed FG-Nups are dispensable [24, 25]. The asymmetrical FG-Nups can even be swapped between the two sides of NE without affecting the active transport [24]. This is mimicked in our model by introducing two types of FG-Nups: binding, $\epsilon < 0$, and non-binding, $\epsilon = 0$, FG-Nups. In Figure 4b it is shown that symmetrically placed FG-Nups (Figure 1b) facilitates active transport roughly like centrally placed FG-Nups (Figure 1a). If the distribution of FG-Nups is asymmetrical, the active transport is hampered, since either the entrance or the exit (or both) of the NPC is blocked by the steric entropic barrier.

The physical model of nuclear pore transport provide some predictions as well. A significant finding is that many, but shorter, FG-Nups are far more effective for the formation of the steric entropic barrier than fewer and longer FG-Nups (Figure 5a). In the model there is an optimal polymer length for the FG-Nups, beyond which the entropic barrier height is not advanced further (Figure 5b). The broadening of the free energy barrier indicates that the FG-Nups extend out of the pore as the length of the FG-Nups is increased, while the density in pore has a maximum set by the grafting density. Overall, this suggests that barrier properties of NPC is set by the number of flexible FG-Nups, while the presence of longer FG-Nups, which tend to be partly squeezed out of the pore, may be important for increasing the affinity

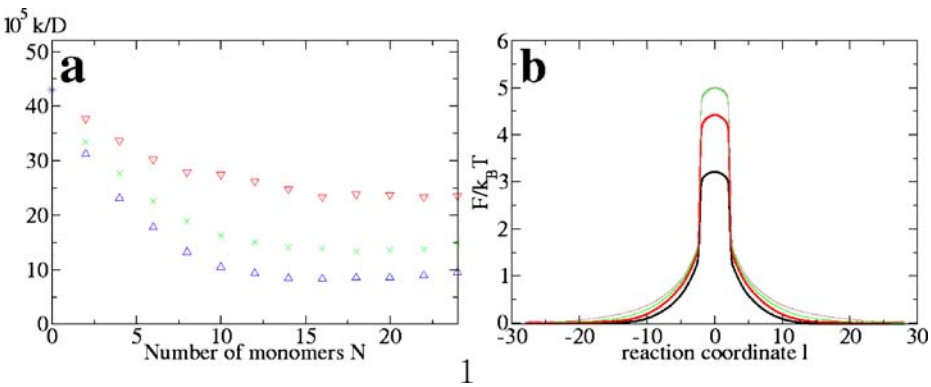

Figure 5 Barrier properties for different FG-Nup occupations of a simple pore (see Figure 1a,c) and $\epsilon = 0$. The cargo-carrier complex consists of 10 monomers. **(a)** Reaction rates versus length (number of monomers) of *centrally placed FG-Nups*. The number of FG-Nups in the pore is 8 (*red points*), 16 (*green*) and 24 (*blue*). The rate is generally decreasing with the length of the FG-Nup until some threshold length (12–14) beyond which it saturates. The saturation rate is determined by the number of FG-Nups in the pore. Comparing the pore configurations with equal amounts of monomers, e.g. eight FG-Nups of length 20 and 16 FG-Nups of length 10, it is observed that more and shorter FG-Nups form a more effective barrier than fewer and longer FG-Nups. **(b)** The development of the barriers is shown for 24 FG-Nups in the pore of length 4 (*black curve*), 10 (*red*), 16 (*green*) and 22 (*blue*). A broadening of the steric entropic barrier indicates that the FG-Nups expand out of the pore for long FG-Nups, leaving the density in the pore unchanged.

range around the pore. For further investigations of the structure of the FG-Nups in the pore, complementary Monte Carlo techniques are necessary. Finally, the fact that symmetrically placed FG-Nups facilitate active transport roughly like centrally placed FG-Nups (Figure 1a) in our model indicates that Nature has an extensive liberty in the design of the NPC to facilitate active transport of macromolecules.

4 Conclusion

From a model calculation we have demonstrated that a very simple buildup of the NPC provides for a mechanism of active nuclear pore transport, which can explain and account for most observed characteristics: the barrier properties of NPC for macromolecules in general, the barrier reducing role of the affinity of cargo-carrier complexes to NPC, the selectivity of the active transport across the NPC, the possibility of parallel transport pathways where different FG-Nups or combinations of them facilitates the transport of selected carrier proteins and deleting or swapping asymmetric FG-Nups have minor effects on the active transport through NPC. It has been demonstrated that a single structure can facilitate both the barrier and the affinity of cargo-carrier complexes to the NPC and the transport mechanism. Given the simplicity of this structure, we expect that Nature has adopted it for other active transport and filtration purposes involving macromolecules. Furthermore, we expect that a model system of NPC, which can provide active transport easily can be realized experimentally with modern surface and polymer grafting techniques [4, 26].

Note A referee has made us aware of a new publication by Lim et al. [26], which demonstrate that the FG-Nup Nup153 in cytosol buffer conditions behaves as a flexible polymer in a good solvent: in single molecule force spectroscopy by Atomic Force Microscropy (AFM) it shows worm-like chain behavior with a persistence length about 4 Å under extension, and in colloidal force measurements with AFM a surface grafted with Nup153 displayed steric entropic repulsion. Our key assumption of FG-Nups as random coil polymers in good solvent is thus strongly supported in this experimental work along with evidence for the steric, entropic nature of the barrier for passive transport of macromolecules through NPC.

Acknowledgements MEMPHYS—Centre for Biomembrane Physics is supported by the Danish National Research Foundation. The numerical analysis was supported by a grant from the Danish Center for Scientific Computing.

References

1. Görlich, D., Kutay, U.: Transport between the cell nucleus and the cytoplasm. Ann. Rev. Cell Dev. Biol. **15**, 607–660 (1999)
2. Rowat, A.C., Foster, L., Weiss, M., Nielsen, M., Ipsen, J.H.: Biophysical studies of the cell nucleus: physical properties of the nuclear lamina. J. R. Soc. Interface **2**, 63–69 (2005)
3. Rout, M.P., Aitchison, J.D., Suprapto, A., Hjertaas, K., Zhao, Y.: The yeast nuclear pore complex: composition, architecture, and transport mechanism. J. Cell Biol. **148**, 635–651 (2000)
4. Lim, R.Y.H., Aebi, U., Stoffler, D.: From the trap to the basket: getting to the bottom of the nuclear pore complex. Chromosoma **115**, 15–26 (2006)

5. Denning, D.P., Patel, S.S., Uversky, V., Fink, A.L., Rexach, M.: Disorder in the nuclear pore complex: the FG repeat regions are natively unfolded. Proc. Natl. Acad. Soc. **100**, 2450–2455 (2003)
6. Fahrenkrogh, B., Köser, J., Aebi, U.: The nuclear pore complex: a jack of all trades? Trends Biochem. Sci. **29**, 175–182 (2004)
7. Yang, W., Gelles, J., Musser, S.M.: Imaging of single-molecule translocation through nuclear pore complexes. Proc. Natl. Acad. Soc. **101**, 12887–12892 (2004)
8. Feldherr, C.M., Akin, D.: The location of the transport gate in the nuclear pore complex. J. Cell. Sci. **110**, 3065–3070 (1997)
9. Elbaum, M.: The nuclear pore complex: biochemical machine or Maxwell demon? C. R. Acad. Sci. Paris **2**, 861–870 (2001)
10. Suntharalingam, M., Wente, S.: Peering through the Pore: nuclear pore complex structure, assembly, and function. Dev. Cell **4**, 775–789 (2003)
11. Timney, B.L., Rout, M.P.: Robbing from the pore. Nat. Cell Biol. **6**, 177–179 (2004)
12. Bickel, T., Bruinsma, R.: The nuclear pore complex mystery and anomalous diffusion in reversible gels. Biophys. J. **83**, 3079–3087 (2002)
13. Kustanovich, T., Rabin, Y.: Metastable network model of protein transport through nuclear pores. Biophys. J. **86**, 2008–2016 (2004)
14. Kramers, H.A.: Brownian motion in a field of force and the diffusion model of chemical reactions. Physica **7**, 284–304 (1940)
15. Grabert, H.: Projection operator techniques in nonequilibrium statistical mechanics. Springer Tracts in Modern Physics, vol. 95. Springer, Berlin (1982)
16. Chattopadhyay, K., Elson, E.L., Frieden, C.: The kinetics of conformational fluctuations in an unfolded protein measured by fluorescence methods. Proc. Natl. Acad. Sci. **102**, 2385–2389 (2005)
17. Reimann, P., Schmid, G.J., Hänggi, P.: Universal equivalence of mean first-passage time and Kramers rate. Phys. Rev. **60**, R1–R4 (1999)
18. Görlich, D., Pante, N., Kutay, U.: Identification of different roles for RanGDP and RanGTP in nuclear protein import. EMBO J. **15**, 5584–5594 (1996)
19. Matsuura, Y., Lange, A., Harreman, T.M., Corbett, A.H., Stewart, M.: Structural basis for Nup2p function in cargo release and karyopherin recycling in nuclear import. EMBO J. **22**, 5358–5369 (2003)
20. Lee, J.: New Monte Carlo algoritm: entropic sampling. Phys. Rev. **71**, 211–214 (1993)
21. Wang, F., Landau, D.P.: Efficient, multiple-range random walk algoritm to calculate the density of states. Phys. Rev. Lett. **86**, 2050–2053 (2001)
22. Kubitscheck, U., Grünwald, D., Hoekstra, A., Rohleder, A., Kues, T., Siebrasse, J.P., Peters, R.: Nuclear transport of single molecules: dwell times of the nuclear pore complex. J. Cell Biol. **168**, 233–243 (2005)
23. Goldfarb, D., Michaud, N.: Pathways for the nuclear transport of proteins and RNAs. Trends Cell Biol. **1**, 20–24 (1991)
24. Zeitler, B., Weis, K.: The FG-repeat asymmetry of the nuclear pore complex is dispensable for bulk nucleocytoplasmic transport in vivo. J. Cell Biol. **167**, 583–590 (2004)
25. Strawn, L.A., Shen, T., Shulga, N., Goldfarb, D.S., Wente, S.: Minimal nuclear pore complexes define FG repeat domains essential for transport. Nat. Cell Biol. **6**, 197–206 (2004)
26. Lim, R.Y.H., Huang, N., Köser, J., Deng, J., Lau, K.H.A., Schwarz-Herion, K., Fahrenkrog, B., Aebi, U.: Flexible phenylalanine–glycine nucleoporins as entropic barriers to nucleocytoplasmic transport. Proc. Natl. Acad. Sci. **103**, 9512–9517 (2006)